JACS
JOURNAL OF THE AMERICAN CHEMICAL SOCIETY
Article
pubs.acs.org/JACS

Mechanically Tightening a Protein Slipknot into a Trefoil Knot

Chengzhi He,[†] Guillaume Lamour,[‡] Adam Xiao,[†] Joerg Gsponer,[‡] and Hongbin Li*[,†]

[†]Department of Chemistry, University of British Columbia, Vancouver, BC V6T 1Z1, Canada
[‡]Center for High Throughput Biology, University of British Columbia, Vancouver, BC V6T 1Z1, Canada

Supporting Information

ABSTRACT: The knotted/slipknotted polypeptide chain is one of the most surprising topological features found in certain proteins. Understanding how knotted/slipknotted proteins overcome the topological difficulty during the folding process has become a challenging problem. By stretching a knotted/slipknotted protein, it is possible to untie or tighten a knotted polypeptide and even convert a slipknot to a true knot. Here, we use single molecule force spectroscopy as well as steered molecular dynamics (SMD) simulations to investigate how the slipknotted protein AFV3-109 is transformed into a tightened trefoil knot by applied pulling force. Our results show that by pulling the N-terminus and the threaded loop of AFV3-109, the protein can be unfolded via multiple pathways and the slipknot can be transformed into a tightened trefoil knot involving ~13 amino acid residues as the polypeptide chain is apparently shortened by ~4.7 nm. The SMD simulation results are largely consistent with our experimental findings, providing a plausible and detailed molecular mechanism of mechanical unfolding and knot tightening of AFV3-109. These simulations reveal that interactions between shearing β-strands on the threaded and knotting loops provide high mechanical resistance during mechanical unfolding.

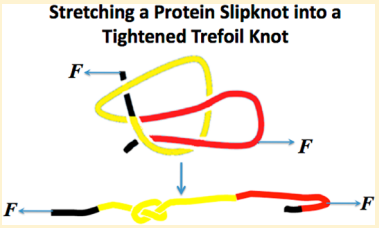

INTRODUCTION

Proteins exhibit the remarkable ability of navigating themselves on a complex energy landscape to achieve robust and fast folding.[1−4] Knotted structures within folded proteins were previously considered impossible due to the enormous topological difficulty during protein folding process.[5] Indeed, most proteins do not possess knotted topologies. Stretching such proteins will fully extend them to linear polypeptide chains without any knots. However, the development of bioinformatics tools has revealed that proteins do exhibit these more complex topologies, where approximately 1% of proteins in the protein data bank contain knotted or slipknotted backbones.[5−9] The knot types vary from the simplest trefoil knot (3_1 knot) to complex Stevedore's knot (6_1 knot).[6] Web servers have been established to detect knots in protein structures, and we can expect that the number of knotted proteins will continue to grow.[10−12] Although there is still debate as to whether and how the knotted topology relates to biological functions, recent studies have shown that knotted regions are important to both ligand binding and enzyme activity.[8,13−16] Despite their complex topology, these knotted or slipknotted proteins can spontaneously fold into their native conformations in order to carry out their specific biological functions.[2,6−8,15−20] Understanding how proteins fold into such complex knotted or slipknotted structures has attracted considerable interests over the past few years. Experimental and simulation efforts have started to offer insights into the molecular mechanisms of these complex folding processes.[6,8,13,15,16,19−30] Experimental studies have shown that although knotted proteins can acquire their native knotted topology spontaneously, molecular chaperones inside the cell can speed up the folding process of such knotted proteins.[28] Simulation studies suggested that the formation of a slipknot structure can serve as an important intermediate step to reduce the topological difficulty as knotted proteins fold.[8,16,19] However, it is difficult to test this prediction experimentally, because such a slipknot intermediate lacks most tertiary structure of a folded knotted protein and is difficult to detect its formation and conversion into a true knot in experiments. In contrast to such slipknot intermediate states, slipknot proteins assume well-defined slipknotted structures with fully formed secondary and tertiary structure in their native state, which can be detected readily in experiments. Simulation studies revealed that by pulling a knotted protein from different directions, it is possible to untie a knot or tighten a knot.[31] Similarly, it should be feasible to untie a slipknot or convert a slipknot into a true knot by pulling a slipknot from appropriate directions. Tying a slipknot into a true knot could offer insights that are relevant for understanding the mechanism and energetics for the conversion of a slipknotted intermediate to a knotted structure, despite that slipknotted proteins are not ideal model systems for testing the proposed slipknot intermediate mechanism. Moreover, tying a slipknot into a tightened knot will provide an invaluable opportunity to study the refolding process of a slipknotted protein starting from a tightened knot state, which is similar to the reverse process for the knot-forming process from a slipknot intermediate state. Here, we use a small slipknotted protein AFV3-109 (PDB code 2J6B)[32] as a model system to study the conversion of a slipknotted protein into a trefoil knotted structure upon stretching by combining protein engineering, atomic force microscopy (AFM)-based single molecule force spectroscopy,

Received: April 22, 2014
Published: August 4, 2014

   dx.doi.org/10.1021/ja503997h | J. Am. Chem. Soc. 2014, 136, 11946−11955

and steered molecular dynamics simulations (SMD) techniques.

AFV3-109 (PDB code 2J6B) is a small protein with a slipknot topology. As shown in Figure 1, a knotting loop is formed near the N- terminus (colored in yellow) of AFV3-109, where a threaded loop near the C-terminus (colored in red) is inserted into the knotting loop. Just like a shoelace, the protein slipknot can be untied or converted into a tightened knot depending on where pulling force is applied. Previous studies confirmed that slipknotted AFV3-109 can be untied and fully extended to a linear polypeptide chain by pulling the protein from its N- and C-termini.[33] If one pulls the threaded loop of AFV3-109, it is possible to pull the threaded loop through and into the knotting loop to convert a slipknot into a true knot. Using protein engineering techniques, we engineered a cysteine variant Lys98Cys of AFV3-109 that allows us to stretch AFV3-109 from the N-terminus and residue Cys98. Our results show that by pulling on the N-terminus and the threaded loop of AFV3-109, the protein can be mechanically unfolded via multiple pathways and the slipknot can be converted into a tightened trefoil knotted structure, which involves ∼13 amino acid residues and leads to a shortening of the fully extended polypeptide chain by ∼4.7 nm. SMD simulations revealed unfolding pathways that are consistent with these experimental results, and provided a plausible molecular mechanism underlying the unfolding of the slipknotted structure.

MATERIALS AND METHODS

Protein Engineering. The gene encoding wild-type AFV3-109 was purchased from Genescript. The cysteine variant of AFV3-109 (K98C) was constructed using standard site-directed mutagenesis methods. K98C was then subcloned into a $(GB1)_4$-pQE80L vector encoding the polyprotein $(GB1)_4$ gene to obtain $(GB1)_4$-K98C.[34] $(GB1)_4$-K98C was overexpressed in DH5α strain induced by isopropyl β-D-1-thiogalactopyranoside (IPTG). A Co^{2+} affinity column was used for protein purification. Proteins were stored at 4 °C in phosphate buffered saline (PBS) solution at a protein concentration from 2 to 6 mg/mL. The full sequence of $(GB1)_4$-K98C, which contains an N-terminal His-tag, is as follows:

MRGSHHHHHHGS(MDTYKLILNGKTLKGETTTEAVDA-ATAEKVFKQYANDNGVDGEWTYDDATKTFTVTERS)$_4$**MLYILN-SAILPLKPGEEYTVKAKEITIQEAKELVTKEQFTSAIGHQAT-AELLSSILGVNVPMNRVQIKVTHGDRILAFMLKQRLPEGVVV-KTTEELECIGYELWLFEIQRS**

The sequence in italic corresponds to $(GB1)_4$ and the sequence in bold corresponds to the K98C variant of AFV3-109. Residue Cys98 is underlined.

Single Molecule Force Spectroscopy. Single molecule force spectroscopy experiments were carried out on a homemade AFM[35] as well as commercially available AFMs (Cypher and MFP3D AFM from Asylum Research). Before each experiment, we calibrated the spring constant (which ranged from 30 to 50 pN/nm) of each individual AFM cantilever (Si_3N_4 cantilevers from Bruker) using the equipartition theorem.[7] In a typical AFM experiment, we deposited ∼1.0 μL of protein solution (1.0 mg/mL) in PBS onto a clean glass cover slip covered by PBS buffer (∼50 μL) and allowed the protein to adsorb onto the substrate for ∼10 min before force spectroscopy experiments. Data analysis was accomplished using custom written codes in IGOR Pro 6.0. We used worm-like chain (WLC) model of polymer elasticity[36] to fit consecutive unfolding force peaks to obtain the contour length increment upon domain unfolding. A persistence length of 0.4 nm, which is typical for unfolded polypeptide chain, was used in all WLC fitting.

Monte Carlo Simulations. The mechanical unfolding of mutant K98C was described using the Bell-Evans model.[37,38] The force-dependent unfolding rate constant can be described as $\alpha(F) = \alpha_0 \exp(F\Delta x_u/k_BT)$, where $\alpha(F)$ is the unfolding rate constant at external force of F, α_0 is the unfolding rate constant at zero force, Δx_u is the distance from native state and transition state, k_B is the Boltzmann constant, and T is the temperature in Kelvin. We carried out Monte Carlo simulations according to previously described procedures[39,40] to estimate the kinetic parameters α_0 and Δx_u, which describe the mechanical unfolding of K98C.

Steered Molecular Dynamics Simulations. Constant force and constant velocity SMD simulations were performed using NAMD[41] and CHARMM22 force field[42] with CMAP correction.[43] The structure of K98C was obtained by mutating the wild-type AFV3-109 (PDB code: 2J6B) using Visual Molecular Dynamics (VMD).[44] The protein was solvated using FACTS, an implicit solvent environment, and the ensemble was NVT.[45,46] The system was energetically minimized and equilibrated for 1 ns before applying pulling force on the N-terminus and residue 98. Pulling forces varied from 800 to 1500 pN in constant force mode, and pulling velocity ranged from 1×10^8 to 5×10^{10} nm/s in constant velocity mode. Three trajectories were obtained at each constant pulling velocity and constant force, with the exception that at constant force of 1200 pN, 20 trajectories were obtained. VMD and IGOR Pro were used for data analysis.

RESULTS AND DISCUSSION

Tightening the Slipknot into a Trefoil Knot Involving ∼13 Amino Acid Residues. To study the mechanical tightening of the protein slipknot located in AFV3-109, we mutated residue 98 located in the threaded loop (colored in red, Figure 1) into a cysteine residue and fused K98C to the C-terminus of the polyprotein $(GB1)_4$. We found that residue Cys98 can be readily oxidized to form a disulfide bond between two neighboring $(GB1)_4$-K98C molecules to form the dimer $(GB1)_4$-K98C−K98C-$(GB1)_4$ (Supporting Information Figure S1). The formation of $(GB1)_4$-K98C−K98C-$(GB1)_4$ made it possible to stretch the slipknotted protein AFV3-109 from its N-terminus and residue Cys98 to convert the slipknot structure into a tightened trefoil knot structure. In this construct, well-characterized GB1 domains, which unfold at ∼180 pN at a pulling speed of 400 nm/s with a contour length increment (ΔLc) of 18 nm,[34,35] serve as fingerprint domains for identifying single molecule stretching events and the mechanical unfolding signature of K98C.

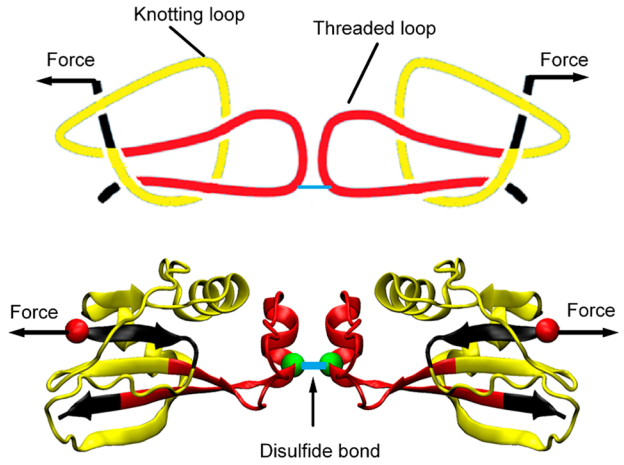

Figure 1. Schematic showing K98C as it is pulled from its N-terminus and residue 98. The threaded loop is colored in red and the knotting loop in yellow. A disulfide bond can be formed by oxidizing residue Cys98, making it possible to stretch AFV3-109 from its N-terminus and residue Cys98.

Stretching $(GB1)_4$-K98C−K98C-$(GB1)_4$ resulted in force−extension curves that exhibited a characteristic sawtooth pattern

dx.doi.org/10.1021/ja503997h | J. Am. Chem. Soc. 2014, 136, 11946−11955

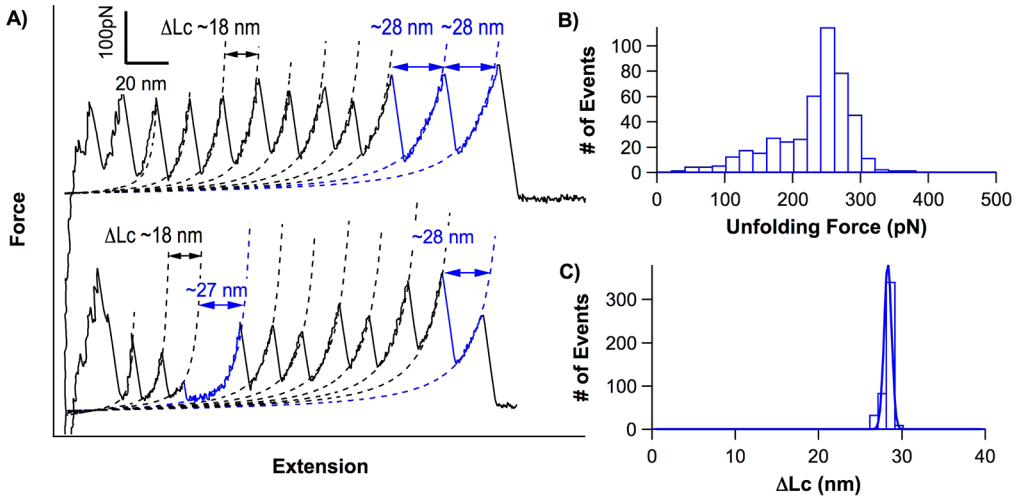

Figure 2. Majority of K98C unfold in a two-state fashion via pathway I. (A) Representative force−extension curves of $(GB1)_4$-K98C−K98C-$(GB1)_4$. Dotted lines correspond to WLC fits to the experimental data. A persistence length of 0.4 nm was used in the WLC fitting. GB1 unfolding events are characterized by an unfolding force of ~180 pN and ΔLc of 18 nm, and are colored in black. Unfolding events of K98C are characterized by a ΔLc of ~28 nm and colored in blue. (B) Unfolding force histogram of K98C at a pulling speed of 400 nm/s in the two-state unfolding pathway. The average unfolding force of K98C at 400 nm/s is 244 ± 35pN (average ± standard deviation, n = 467). (C) ΔLc histogram of K98C in the two-state unfolding pathway. Gaussian fit to the experimental data measures an average ΔLc of 27.8 ± 0.5 nm (n = 467).

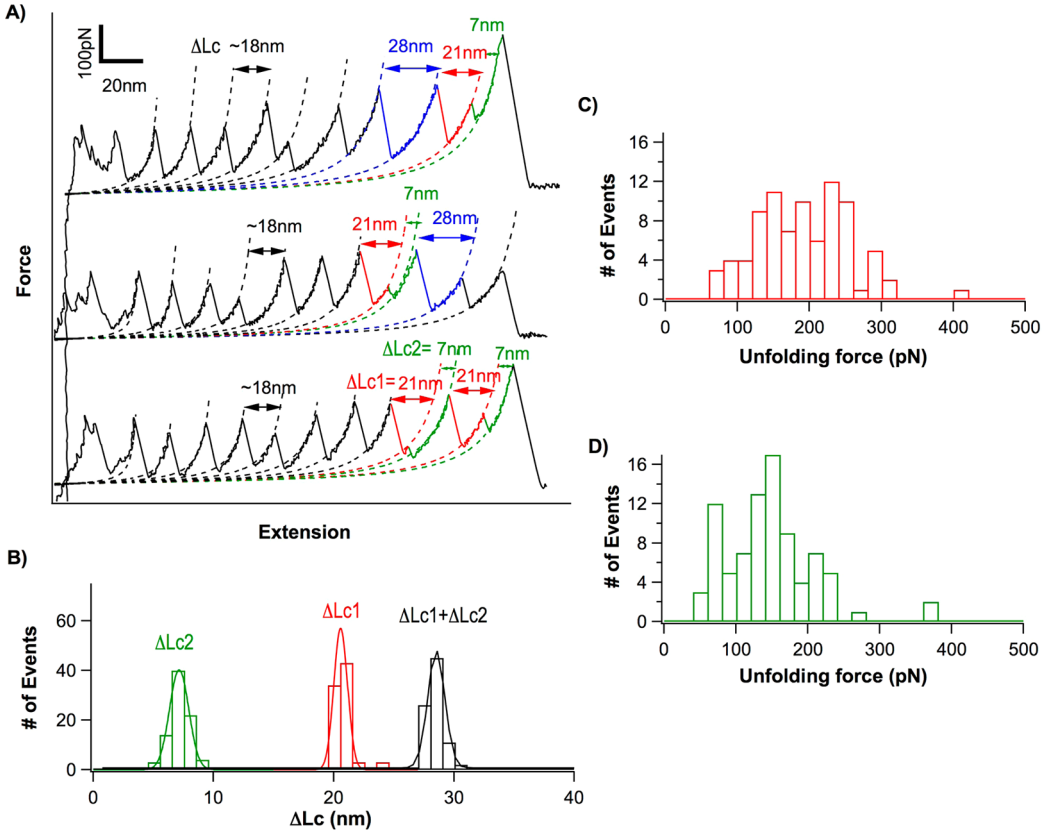

Figure 3. K98C can unfold via a three-state pathway (pathway II) involving an unfolding intermediate I. (A) Representative force extension curves of $(GB1)_4$-K98C−K98C-$(GB1)_4$ involving the formation of the intermediate I for K98C. GB1 unfolding events are colored in black, and two-state unfolding events are colored in blue. Three-state unfolding events of N−I and I−U in K98C are colored in red and green. Dotted lines show WLC fits to the experimental data. (B) The contour length increment histogram for the three-state unfolding of K98C through intermediate I. Gaussian fits (solid lines) to the experimental data measure ΔLc1 of 20.8 ± 0.7 nm (n = 85), ΔLc2 of 7.2 ± 1.1, and the sum ΔLc1 + ΔLc2 of 27.8 ± 0.7 nm, respectively. (C and D) Unfolding force histograms of N−I (red) and I−U (green) in three-state unfolding of K98C. The average unfolding force for N−I is 200 ± 64 pN, and 158 ± 62 pN for I−U (n = 85).

appearance (Figure 2A), where each sawtooth corresponds to the mechanical unfolding of one domain in the polyprotein chain; the last peak typically corresponds to the detachment of the polypeptide chain from either the AFM tip or the substrate.

dx.doi.org/10.1021/ja503997h | J. Am. Chem. Soc. 2014, 136, 11946−11955

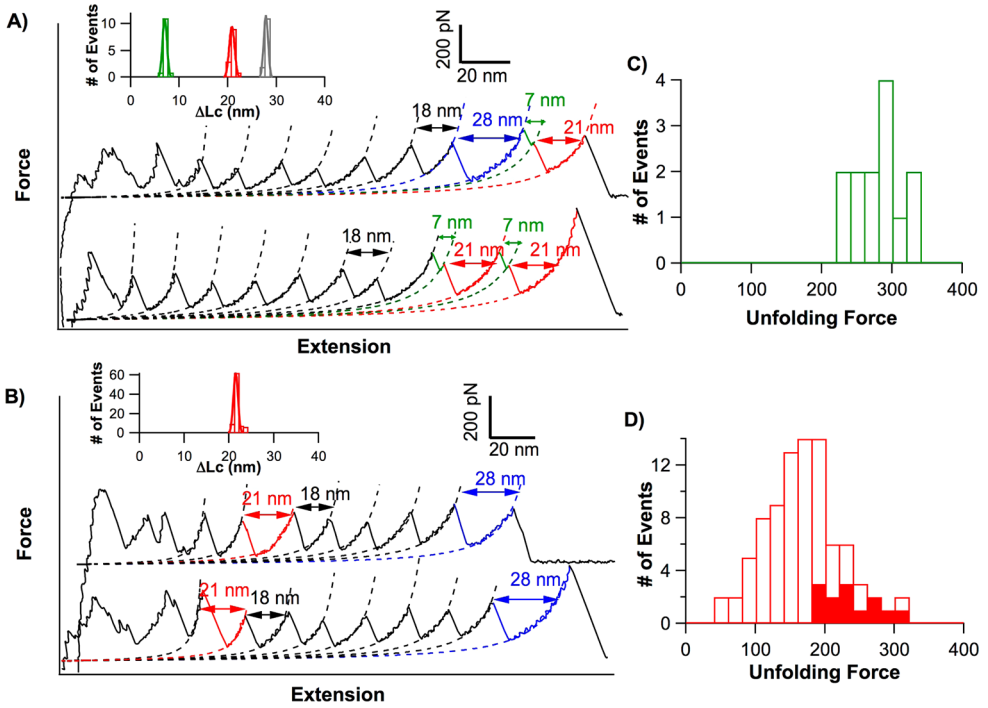

Figure 4. A small percentage of K98C unfolds in three-state fashion involving the formation of an unfolding intermediate II. (A) Representative force extension curves of $(GB1)_4$-K98C–K98C-$(GB1)_4$ with N–II–U three state unfolding of K98C. GB1 unfolding events are colored in black, and two-state K98C unfolding events are colored in blue. Unfolding events of N–II and II–U during the three-state unfolding of K98C are colored in green and red, respectively. The inset shows ΔLc histograms for the three-state unfolding events. Gaussian fits (solid lines) to the experimental data measure ΔLc1 of 7.0 ± 0.5 nm (n = 13), ΔLc2 of 20.8 ± 0.6 nm, and the sum ΔLc1 + ΔLc2 of 27.8 ± 0.5 nm, respectively. (B) Representative force–extension curves showing unfolding events of II–U only. The inset shows the ΔLc histogram. Gaussian fit measures an average ΔLc2 of 21.0 ± 0.7 nm (n = 87). (C and D) Unfolding force distribution histograms of N–II (green) and II–U (red) in three-state unfolding of K98C. The red solid bars are from II–U events in complete N–II–U pathway and red open bars are from II–U only events. The average unfolding force for N–II is 282 ± 37 pN (n = 13), 176 ± 58 pN for all II–U events (n = 100).

Fitting these unfolding force peaks using the worm-like chain model[36] of polymer elasticity revealed the contour length increment (ΔLc) upon domain unfolding. Unfolding events that occur at ∼180 pN with a ΔLc of ∼18 nm correspond to the unfolding of GB1 fingerprint domains (colored in black).[34,35] As two K98C domains are flanked by $(GB1)_4$ repeats in the disulfide bonded dimer $(GB1)_4$-K98C–K98C-$(GB1)_4$, we can ensure that the two K98C domains have been stretched and extended if five or more GB1 unfolding events are observed.[47] As shown in Figure 2A, we observed two additional unfolding events with a ΔLc of ∼28 nm and an unfolding force of ∼240 pN (colored in blue) in addition to the GB1 unfolding events (seven for the top trace and eight for the bottom trace). These two unfolding events can thus be readily attributed to the unfolding of the slipknotted protein K98C. Most K98C unfolding events occur after GB1 domains have been unfolded (top trace, Figure 2A), suggesting that K98C is mechanically more stable than GB1. Indeed, the average unfolding force of K98C is ∼240 pN at a pulling speed of 400 nm/s, higher than that of GB1 (∼180 pN) (Figure 2B). It is of note that due to the stochastic nature of mechanical unfolding, it is possible that some K98C unfolding events occur before all GB1 domains have unfolded (bottom trace, Figure 2A). The unfolding of K98C occurs as a single step with a ΔLc of ∼28 nm, suggesting that the unfolding of K98C occurs in an all-or-none (two-state) fashion (Figure 2C). We term this pathway as pathway I. In addition, the large ΔLc observed during the mechanical unfolding of K98C suggests that most of the tertiary and secondary structure of K98C unravels during this process. ∼72% of the unfolding events of K98C follow this two-state pathway.

As the force is applied on residues 1 and 98 in K98C, the fully extended length of the polypeptide chain would be 35.8 nm if there were no knotted structure (98 aa × 0.365 nm/aa). The distance between residue 1 and 98 in the native state is 3.1 nm. Thus, the complete unfolding of K98C would result in a ΔLc of ∼32.7 nm if there were no knot formation. The experimentally observed ΔLc of ∼28 nm is ∼4.7 nm shorter than the expected ΔLc without a knot. This ∼4.7 nm shortening, which corresponds to ∼13 residues, can be attributed to the formation of a tightened knot. This result clearly indicates that upon stretching from residues 1 and 98, the slipknot structure in AFV3-109 does not get untied. Instead, the slipknot is pulled into a tightened knot, corresponding to the simplest trefoil knot (3_1 knot).

Slipknot Tightening Can Be Accomplished through Multiple Pathways, While the Size of the Tightened Knot Remains the Same. In addition to the predominant two-state unfolding of K98C, we also observed that the unfolding of K98C and the tightening of the trefoil knot can occur following multiple different pathways, involving the formation of intermediate states. As shown in Figure 3A, the unfolding of K98C domains occurs in two steps, giving rise to unfolding events with a ΔLc1 of ∼21 nm for the first step, and a ΔLc2 of ∼7 nm for the second step (Figure 3B, red and green histograms). This result suggests that unfolding of K98C involves the formation of an intermediate state.

dx.doi.org/10.1021/ja503997h | J. Am. Chem. Soc. 2014, 136, 11946–11955

In this pathway (termed as pathway II), the native state is more mechanically resistant than the intermediate state, and unfolds with an average force of ∼200 pN (Figure 3C), while the unfolding of the intermediate state, which is termed as "intermediate I", occurs at ∼160 pN (Figure 3D). This timing of a higher unfolding force peak followed by a lower force peak is indicative of a reverse mechanical hierarchy, suggesting that the mechanical unfolding intermediate state is protected by the native structure and is subject to the stretching force only after the native state has been partially unraveled. In addition, it is noteworthy that the sum of ΔLc1 and ΔLc2 (∼28 nm, Figure 3B) is the same as that for the two-state unfolding pathway, suggesting that this three-state unfolding pathway also leads to the formation of a similar tightened trefoil knot structure when K98C is unfolded and extended to higher extensions. This three-state unfolding pathway occurs at a frequency of ∼13%.

Interestingly, a small percentage of K98C domains (∼2%) unfold through a different three-state unfolding pathway (termed as pathway III, Figure 4A). Initial unfolding of K98C results in unfolding events with a ΔLc of ∼7 nm, followed by a second unfolding step of ΔLc of ∼21 nm, which corresponds to the unfolding of a different intermediate state. We termed this intermediate as "intermediate II". The sum of the ΔLc1 and ΔLc2 is 28 nm (Figure 4B), suggesting that this unfolding pathway also leads to the formation of a tightened trefoil knot structure that is similar in size to that encountered in the first two pathways. Unfolding forces for the two steps in this pathway are shown in Figure 4C,D.

In addition to the observed pathways I−III, we also observed a significant fraction of K98C unfolding events (∼13%) show only ΔLc of ∼21 nm (Figure 4B), suggesting that the unfolding of K98C began from the unfolding intermediate state II as in the pathway III. It is likely that part of K98C in the native state unfolded at low forces, making the initial unfolding undetectable because the force is below the force detection limit of our AFM or such low force events are buried in the region of force−extension curves dominated by nonspecific interactions (Figure 4B). Thus, the unfolding events displaying only ΔLc of ∼21 nm likely follow a pathway similar to unfolding pathway III, except that the initial unfolding step of ΔLc of ∼7 nm occur at much lower forces. It is of note that the unfolding force histogram of II−U in the complete N−II−U pathway matches the high force part of the distribution from the II−U only events (Figure 4D). For simplicity, we consider both types of unfolding events (7 nm event followed by 21 nm, and 21 nm only events) as events following pathway III, which amount to 15% in all unfolding events of K98C.

The ΔLc of pathway III is indistinguishable from that ascribed to pathway II; however, it is unknown whether similar structural elements are responsible for the similar ΔLc exhibited by the two unique three-state unfolding pathways.

Multiple Pathways Reveal a Kinetic Partitioning Mechanism for Mechanical Unfolding. Our results demonstrate that the mechanical unfolding of the slipknotted protein variant K98C proceeds via multiple parallel pathways, which all result in the tightening of the slipknot into a trefoil structure. Approximately 72% of K98C unfolded through a two-state unfolding pathway (pathway I), with ∼13% occurring through intermediate I (pathway II) and ∼15% through intermediate II (pathway III). These results are in agreement with the kinetic partitioning mechanism[47,48] for protein folding and unfolding, which suggests that kinetic traps on the energy landscape can lead to the bifurcation of folding/unfolding pathways and the formation of intermediate states.

To further investigate the unfolding kinetics of K98C, we performed force−extension experiments at different pulling speeds. In our experiments, we did not see obvious effect of pulling speed on the partitioning of different unfolding pathways. Figure 5 shows effect that pulling speed has on

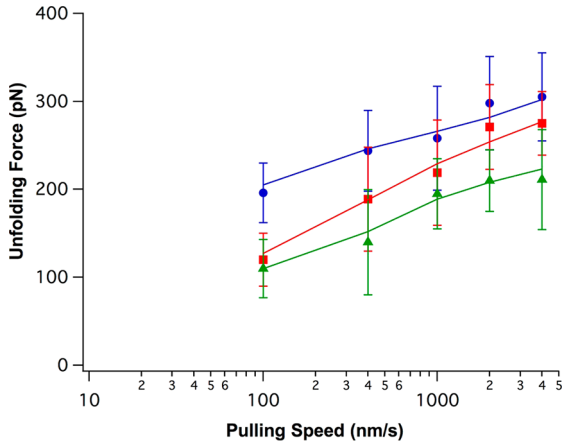

Figure 5. Pulling speed dependence of K98C unfolding. Two-state unfolding events are colored in blue, and three-state unfolding events (with intermediate I) are colored in green and red. Solid lines are Monte Carlo simulation results using kinetic parameters tabulated in Table 1

unfolding forces exhibited by pathways I and II. To estimate the kinetic parameters for different unfolding pathways, we carried out Monte Carlo simulations to reproduce these AFM experiments.[34,39] We found that the kinetic parameters shown in Table 1 can accurately describe our experimental data. Specifically, simulation results show that the unfolding distance to the transition state Δx_u for pathways I and II is small, indicative of how brittle the unfolding transition is.[39] Due to the low frequency of the unfolding step N−II (native to intermediate II) in pathway III, we were not able to obtain a pulling speed dependency or the kinetic parameters for this particular pathway.

K98C Can Refold from a Tightened Trefoil Knot Conformation to Its Native Slipknot Conformation. By stretching AFV3-109 from its N-terminus and residue 98, we stretched a slipknot protein into a tightened trefoil knot. Such a tightened trefoil knot provides an invaluable opportunity to investigate whether a tightened trefoil knot can loosen up to allow the polypeptide to refold into its native slipknot conformation, which involves the conversion of a trefoil knot into a slipknot. To investigate this possibility, we carried out refolding experiments on K98C. First, we stretched K98C to unfold K98C and convert it into a tightened trefoil knot; then we relaxed the unfolded polypeptide chain quickly to zero force and waited 10 s to allow the unfolded protein to refold. We then stretched the protein again to examine whether the K98C has refolded to obtain its native slipknot conformation. Figure 6 shows some force−extension curves from the same molecule during such an experiment. We found that the tightened trefoil knot can refold to the native slipknot conformation of K98C upon the relaxation of the pulling force as judged by the contour length increment ΔLc (indicated by blue stars). However, the probability of successful refolding of K98C to its

dx.doi.org/10.1021/ja503997h | J. Am. Chem. Soc. 2014, 136, 11946−11955

Table 1. Kinetic Parameters of Unfolding Events from Different Pathways[a]

unfolding event		unfolding force (pN)	ΔLc (nm)	Δx_u (nm)	α_0 (s^{-1})	unfolding energy barrier (k_BT)[b]
Pathway I	N−U	244 ± 35	27.7 ± 0.5	0.19	0.0012	20.5
Pathway II	N−I	200 ± 64	20.8 ± 0.7	0.14	0.05	16.8
	I−U	158 ± 62	7.2 ± 1.1	0.16	0.5	14.5
Pathway III	N−II[c]	282 ± 37[d]	7.0	-	-	-
	II−U	176 ± 58[e]	21.0 ± 0.7	0.14	0.05	16.8

[a]ΔLc, contour length increment upon unfolding; Δx_u, distance between the native state and mechanical unfolding transition state; α_0, unfolding rate constant at zero force. Data is represented as average ± standard deviation. [b]Unfolding energy barrier at zero force was estimated based on α_0 assuming a prefactor of 10^6 s^{-1}.[49] [c]Kinetic parameters were not estimated for N−II step in Pathway III due to the small number of events. [d]The average unfolding force was calculated based on unfolding events with clearly identifiable ΔLc1 of 7 nm. The number of events is 13. [e]The average unfolding force was calculated based on all unfolding events with ΔLc2 of 21 nm following Pathway III. The number of events is 100.

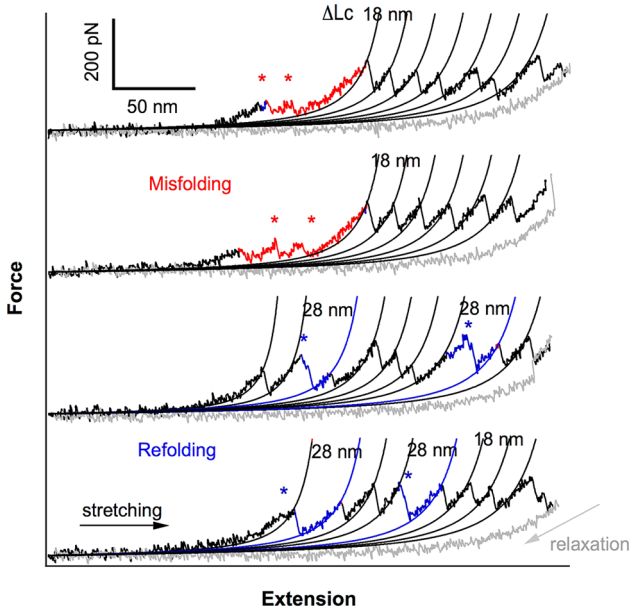

Figure 6. Representative force−extension curves from the same molecule obtained during a refolding experiment. During the refolding experiment, the same polyprotein molecule was stretched to unfold all the domains in the polyprotein chain, and then quickly relaxed to zero force. After waiting for 10 s at zero force to allow the unfolded protein to refold, the protein was stretched again. Unfolding events with ΔLc of 28 nm (colored in blue and indicated by blue stars) correspond to the unfolding of refolded slipknot protein K98C, and unfolding events with ΔLc of 18 nm correspond to the GB1 unfolding events. The unfolding events that give rise to irregular ΔLc (indicated by red stars) are assigned to the unfolding of misfolded K98C domains.

slipknot native state from its trefoil knot conformation is low, as most non-GB1 unfolding force peaks do not show ΔLc of ∼28 nm (indicated by red stars), suggesting that K98C misfolds into conformations other than the native slipknot conformation. These results suggest that the tightened knot does not prevent refolding, but may make the energy landscape more rugged and complex and the protein more prone to misfold.

However, a complete characterization of the refolding behaviors of a tightened knot has not been possible, as such experiments are challenging and require one to hold onto a single molecule for an extended period of time to carry out unfolding and refolding experiments, which is currently beyond the capability of our AFM instruments. More robust and specific attachment chemistry will be required for such refolding experiments and the results will be reported in the future.

SMD Simulations Reveal Molecular Mechanisms for Slipknot Tightening. Single molecule force spectroscopy experimental results reveal complex unfolding behaviors of K98C when its slipknot is tightened into a trefoil knot. To extend K98C, it is necessary to disrupt interactions between different secondary/tertiary structural elements as well as the hydrophobic core; the ΔLc measured during mechanical unfolding of K98C could provide a glimpse of structural elements ruptured during unfolding. To further understand the molecular mechanism underlying multiple unfolding pathways and identify structural elements/interactions critical to the mechanical unfolding of K98C, we carried out SMD simulations under constant pulling velocities as well as constant pulling forces.[41,50,51] Recognizing that the AFM experiments and SMD simulations are carried out at time scales that differ by more than 6 orders of magnitude, we intend to use SMD simulations to obtain a plausible molecular level explanation for our experimental observations and help design new AFM experiments.

When the force is applied between the N-terminus and residue 98 in SMD simulations, β strands β1, β4 and β5 are subject to the applied stretching force, resulting in a bifurcation of unfolding pathways. In the pathway colored in blue (Figure 7), applied steering force caused simultaneous unravelling of parallel β strands $\beta1\beta3\beta4$ and antiparallel strands $\beta4\beta5$ (as evidenced by the disruption of the backbone hydrogen bonds between these β strands), the only major energy barrier between the native and extended tightened knotted state (Figure 8A). During this process, the threaded loop (β strands $\beta4\beta5$) is pulled through the knotting loop, converting the slipknot topology to a trefoil knotted structure. Further stretching causes the loss of remaining secondary structures and tightening of the trefoil knot. It is likely that this trajectory corresponds to the two-state unfolding pathway (pathway I) observed experimentally.

In other trajectories (Figure 7, colored in green and red), the first step corresponds to the unraveling of $\beta1\beta3\beta4$, while interactions between the $\beta4\beta5$ strands remain intact, leading to an extension of ∼7 nm and the formation of an intermediate state (termed as intermediate II′). After this initial energy barrier is surmounted, $\beta2\beta5$ in intermediate II′ is exposed to steering force directly, and unfolding proceeds via two pathways. In the pathway illustrated in red (Figure 8B), intermediate state II′ is short-lived. $\beta2\beta5$ is ruptured and the threaded loop containing the intact $\beta4\beta5$ is pulled through the knotting loop. Further stretching leads to straightening of the helices and unstructured coils, as well as the formation of a tightened trefoil knot while $\beta4\beta5$ remains intact. This intact $\beta4\beta5$ is mechanically resistant, and serves as another

dx.doi.org/10.1021/ja503997h | J. Am. Chem. Soc. 2014, 136, 11946−11955

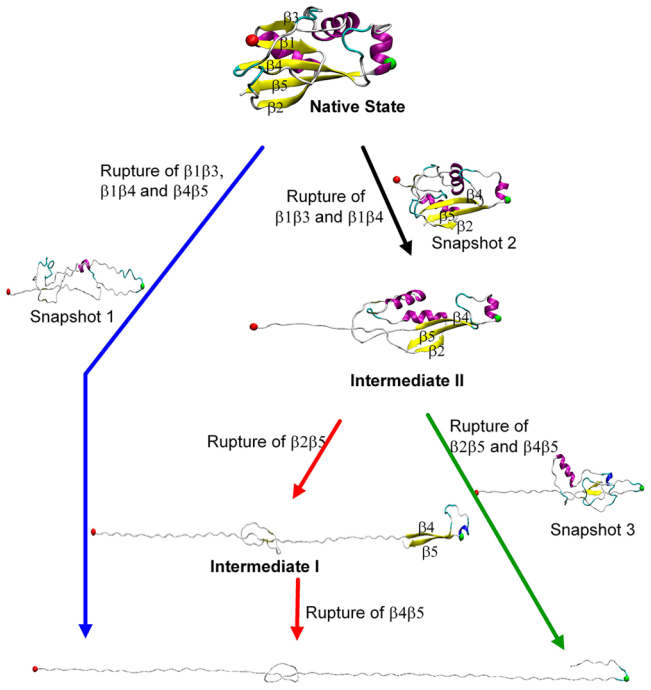

Figure 7. Distinct mechanical unfolding pathways of K98C as observed through SMD simulations. Upon stretching from its N-terminus and residue 98, K98C variant of AFV3-109 unfolds via three distinct unfolding pathways, all of which lead to the conversion of the slipknot into a tightened trefoil knot. Pathway I (colored in blue) corresponds to the two-state unfolding pathway, and pathways II and III (colored in red and green) correspond to unfolding pathways involving distinct unfolding intermediate states. Along each individual unfolding pathway, snapshots of K98C are shown to indicate structural changes occurring for K98C during the unfolding process. Structural elements/interactions that are ruptured during each step of the unfolding process are also indicated.

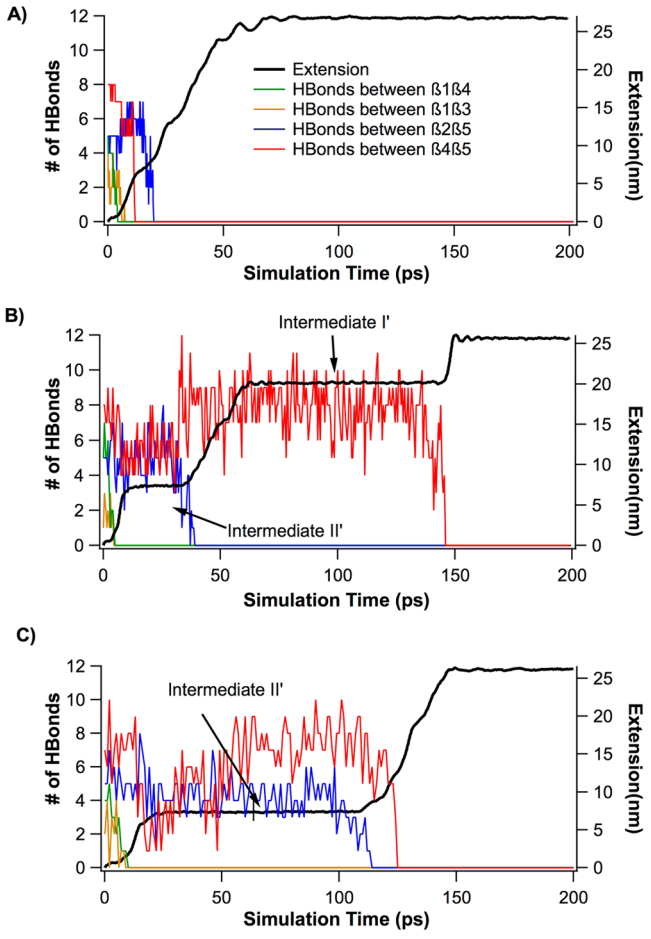

Figure 8. Results of constant force SMD simulations, showing extension and number of hydrogen bonds versus simulation time. (A) Two-state unfolding without intermediate state. (B) Unfolding with two intermediate states. (C) Unfolding with one intermediate state. Unfolding intermediate states manifest themselves as long plateaus in the extension−time curves. The plateau at the extension of ∼26 nm corresponds to the yet to be fully tightened trefoil knot. The three trajectories shown in this figure were run at a constant force of 1200 pN for 200 ps.

intermediate state (we term it intermediate I′). Further stretching resulted in the unraveling of *β4β5* and a further extension of the protein by ∼6 nm.

Figure 8B indicates that energy barriers for this pathway are located at extension of 1, 7, and 20 nm, corresponding to the unravelling of *β3β1β4*, *β2β5*, and *β4β5*, respectively. The intermediate I′ formed at 20 nm extension likely corresponds to the intermediate I observed at ∼21 nm in pathway II in single molecule AFM experiments (Figure 2, colored in red), while the short-lived intermediate II′ is not found in pathway II from experiments. To confirm the link between AFM experiments and SMD simulations, it will be necessary to use loop elongation variants to change the ΔLc of the intermediate state. Such experiments are currently underway and will be reported in the future.[52]

In the pathway colored in green, intermediate state II′ is long-lived (Figure 8C). *β4β5* and *β2β5* provide the major resistance for intermediate II′ to stretching and are broken almost simultaneously. Snapshot 3 shows K98C right before the conversion of the slipknot to a trefoil knot. Further stretching of K98C straightens helices and unstructured coils, and tightens the trefoil knot formed by the polypeptide chain. Figure 8C indicates that the energy barriers located at extension of 1 and 7 nm, corresponds to the unravelling of *β3β1β4* and *β4β5β2*. Intermediate II′ at 7 nm likely corresponds to the intermediate state II observed experimentally in single molecule AFM experiments (Figure 3).

SMD simulation results revealed the number of unfolding pathways and the location of intermediate states, which are largely in agreement with our AFM results, thus providing a plausible molecular mechanism for mechanical unfolding pathways observed experimentally. However, it is important to note that despite the similarity between pathways found in SMD simulations and AFM experiments, the frequency of trajectories in each pathway found in SMD simulations is different from those observed experimentally. Among constant force SMD simulations at 1200 pN, the pathway with intermediate II was encountered ∼85% of the time, while two-state unfolding pathway and the pathway with intermediate I were observed ∼10% and ∼5% of the time, respectively. In contrast, in AFM experiments ∼72% of K98C unfolded through a two-state unfolding pathway, with ∼13% occurring through intermediate I and ∼15% through intermediate II. This difference is likely because SMD simulations are carried out at a time scale that is ∼10^6 to 10^7 times faster than that of AFM experiments. At the SMD simulation time scale, friction within and between polypeptide chains in the protein structure becomes significant, while it is less important at the pulling

dx.doi.org/10.1021/ja503997h | J. Am. Chem. Soc. 2014, 136, 11946−11955

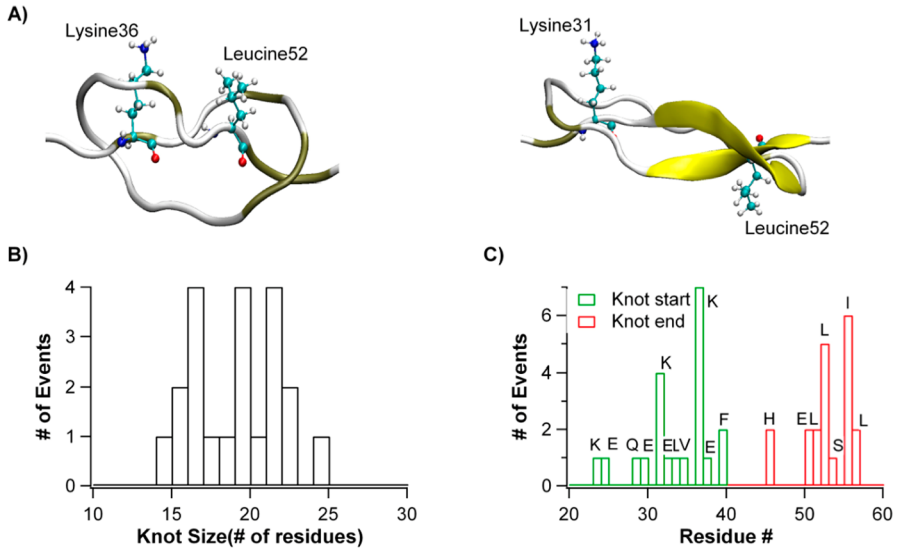

Figure 9. Location and size of tightened knots elucidated through SMD simulations. (A) Snapshots of two tightened knots. We found that the knot described in SMD simulations is not completely tightened. The start and end points of the tightened knot are often residues with bulky side chains. (B) The tightened trefoil knot size histogram. The average size of the tightened trefoil knot in SMD simulations is 20 residues. (C) A histogram of the start and end residues of the tightened trefoil knot.

velocity at which single molecule AFM experiments are performed. It has been suggested that protein unfolding may occur via different mechanisms depending on the pulling velocity.[53] It is uncertain whether the time scale difference between the two techniques is sufficient to explain the difference in trajectory appearance frequency. Ultrafast AFM pulling experiments[53] could possibly bridge the divide between AFM experiments and SMD simulations.

The Size of Tightened Trefoil Knot Is Independent of Unfolding Pathways. Our results from single molecule force spectroscopy experiments showed that the size of the tightened trefoil knot is the same between all unfolding pathways (~13 aa residues in single molecule force spectroscopy experiments). The mechanical tightening of knotted proteins has been studied previously both experimentally and computationally.[54−57] In the study of the mechanical tightening of phytochrome,[55] a protein with a figure-eight knot topology, the size of the tightened figure-eight knot was found to involve ~17 aa residues. It is reasonable to assume that tightened trefoil knot is smaller, considering the difference in knot complexity between the figure-eight knot and the simplest trefoil knot.

SMD simulations also provide key information about the size and location of the tightened trefoil knot within the extended polypeptide chain. Our SMD simulations indicate that the tightening of the trefoil knot is accomplished by shrinking the knotting loop between residues 24 and 56 as shown in Figure 9A. In constant velocity SMD simulations (Supporting Information Figure S2), we found that after overcoming frictions along the pulling process, the trefoil knot became fully tightened at high force (~3000 pN), and the size of the tightened trefoil is ~14 residues, which is in close agreement with that found in AFM experiments (~13 residues). The location of the tightened trefoil knot varies in different trajectories. In addition, constant velocity SMD simulations carried out at different pulling velocity do not show noticeable difference in the molecular events along the unfolding trajectories, but show increased friction experienced by the polypeptide chain at higher pulling velocity.

In contrast to constant velocity SMD simulations, we found that most of the trefoil knots are not fully tightened due to steric hindrance/friction in constant force SMD simulations at 1200 pN. The size of these knots ranges from 14 to 24 amino acid residues (Figure 9B). It is of note that almost all of these knots start and end at residues that have bulky side chain, such as lysine (K), isoleucine (I), glutamic acid (E), leucine (L) (Figure 9C). Evidently, frictions between side chain of these residues and the knotting loop prevent further tightening of the knot. In addition, half of our simulations show that, on knotting loop and threaded loop, the tightened knot forms non-native β-strands, between which the interactions provide further resistance to stretching and prevent further shrinking of the trefoil knot (Figure 9A, right). Previous simulation studies on tightening protein knots showed similar frictions.[55−57]

To further examine the effect of bulky side chain on knot tightening, we mutated K31, K36 and I55, three bulky residues that prevent knot shrinking/sliding in the simulations, with a smaller residue, alanine. The distribution of knot locations becomes broader (Supporting Information Figure S3), which indicates that losing bulky side chain facilitates the sliding of the knot. Thus, it is reasonable to conclude that the bulkier side chains are responsible for preventing the sliding of the knot in the simulation. It is of note that such effect does not exist at the time scale the AFM experiments are performed, because K98C is stretched to a fully tightened trefoil knot (~13 residues) in the AFM experiments.

Major Energy Barriers Do Not Necessarily Arise as a Trefoil Knot Forms from a Slipknot. By correlating our single molecule force spectroscopy experimental results and SMD simulations, we identified three different pathways (N−U, N−I−U, N−II−U), and the likely location of energy barriers/intermediate states along each pathway. As shown in Figure 8, unraveling of $\beta3\beta1\beta4$ is involved in the unfolding of the native state of K98C within all pathways, demonstrating their importance in maintaining the mechanical resistance of the native state of K98C.

In contrast, the key necessary step toward transforming the slipknot to the trefoil knot is to pull threaded loop and the C-

dx.doi.org/10.1021/ja503997h | J. Am. Chem. Soc. 2014, 136, 11946−11955

terminus into the knotting loop, which requires the rupture of $\beta2\beta5$. In the two-state pathway (pathway I) and the three-state pathway (pathway II with ΔLc1 of 21 nm and ΔLc2 of 7 nm), the conversion of the slipknot to a trefoil knot occurs after the major barrier for the unfolding of the native state of K98C (that is the unraveling of $\beta1\beta3\beta4$) has been circumvented, and does not result in any experimentally observable event. Therefore, converting the slipknot to a trefoil knot in these two unfolding pathways (pathways I and II) in the AFM experiments likely does not involve any significant energy barrier. In comparison, in most trajectories following pathway III, the energy barrier for the unfolding of intermediate state II′ corresponds to concurrent rupture of $\beta4\beta5$ and $\beta2\beta5$. Thus, the conversion of the slipknot to a trefoil knot likely contributes to the experimentally observed unfolding energy barrier. Since it is the concurrent rupture of $\beta4\beta5$ and $\beta2\beta5$ that gives rise to the observed energy barrier, which is estimated to be ∼16.8 k_BT assuming a prefactor of 10^6 s^{-1},[49] the barrier caused by rupturing $\beta2\beta5$ alone should be smaller, although we are not able to separate the contributions of rupturing $\beta4\beta5$ from those required for rupturing $\beta2\beta5$. These results suggest that it is possible that topologically converting the slipknot to a trefoil knot does not involve significant energy barrier.

Simulations reported by Sułkowska et al. proposed that forming a slipknot conformation and then threading the end of loop can reduce the topological difficulty of folding into a knotted structure;[8,16,19] thus, slipknot can serve as an important intermediate to facilitate the folding of knotted proteins. It has been challenging to experimentally testing this prediction, because such a slipknot intermediate lacks most tertiary structure of a folded knotted protein and is difficult to detect its formation and conversion into a true knot in experiments. Although AFV3-109 is not an ideal model system for testing this prediction, our results on K98C may nonetheless provide some relevant insights. Compared with the fully structured slipknot of K98C, the proposed slipknot intermediate lacks most tertiary and secondary structure. It can be anticipated that the energy required to convert the "unstructured" slipknot intermediate state to a true knot should be lower than that required for converting the fully structured slipknot in K98C to a trefoil knot. Thus, our results that converting the slipknot in K98C to a trefoil knot does not involve significant energy barrier make the slipknot intermediate mechanism plausible for the folding of knotted proteins. However, it is important to note that if significant contacts were to form between the threading loop and knotting loop in the slipknot intermediate state (as in the case of intermediate state II of K98C) during the folding of a knotted protein, significant energy barrier might arise for converting the slipknot intermediate state to the knotted conformation, leading to a deep kinetic trap that may significantly slow down the folding of the knotted protein.

Furthermore, our AFM experiments also suggest that knot tightening does not increase the mechanical resistance of proteins as compared to unknotted proteins at the time scale the AFM experiments are performed; this may be an important distinguishing feature between AFM experiments and SMD simulations, where friction becomes much more important and tightening a knot could significantly increase the mechanical resistance.

CONCLUSIONS

By combining single molecule AFM and molecular dynamics simulations, we detail the complex mechanical unfolding of a small slipknotted protein AFV3-109, as well as the conversion of its slipknot conformation into a tightened trefoil knot. By stretching AFV3-109 across its N-terminus and residue 98 on the thread loop, we were able to pull the threaded loop through and into the knotting loop, thus converting a slipknot into a true knot. We found that the mechanical unfolding of AFV3-109 can proceed via multiple parallel pathways: AFV3-109 typically unfolds in a two-state fashion, but can unfold through a three-state pathway, involving the formation of distinct intermediate states. During mechanical unfolding, the slipknot is stretched into a tightened trefoil knot, which involves ∼13 amino acid residues and leads to a shortening of the fully extended polypeptide chain by ∼4.7 nm. SMD simulations results confirm unfolding pathways that are consistent with our experimental results, providing a plausible molecular mechanism describing the mechanical unfolding that tightens the trefoil structure. Our study demonstrates that force spectroscopy is a powerful tool to manipulate knotted protein structure, paving the way toward investigating the folding mechanism of highly complex knotted and slipknotted proteins.

ASSOCIATED CONTENT

Supporting Information

Coomassie blue stained sodium dodecyl sulfate polyacrylamide gel electrophoresis (SDS-PAGE) photograph of $(GB1)_4$-K98C; force−extension curves from SMD simulations in constant velocity mode; a figure showing residues with less bulky side chains facilitate the sliding of the knot. This material is available free of charge via the Internet at http://pubs.acs.org.

AUTHOR INFORMATION

Corresponding Author

Hongbin@chem.ubc.ca

Notes

The authors declare no competing financial interest.

ACKNOWLEDGMENTS

This work is supported by the Natural Sciences and Engineering Research Council of Canada, Canada Foundation for Innovation, and Canada Research Chairs Program. This paper is dedicated to the late Professor Charles A. McDowell of UBC.

REFERENCES

(1) Guo, Z. Y.; Thirumalai, D. *Biopolymers* **1995**, *36*, 83.
(2) Onuchic, J. N.; LutheySchulten, Z.; Wolynes, P. G. *Annu. Rev. Phys. Chem.* **1997**, *48*, 545.
(3) Thirumalai, D.; Klimov, D. K.; Woodson, S. A. *Theor. Chem. Acc.* **1997**, *96*, 14.
(4) Onuchic, J. N.; Wolynes, P. G. *Curr. Opin. Struct. Biol.* **2004**, *14*, 70.
(5) Mansfield, M. L. *Nat. Struct. Biol.* **1994**, *1*, 213.
(6) Taylor, W. R. *Nature* **2000**, *406*, 916.
(7) King, N. P.; Yeates, E. O.; Yeates, T. O. *J. Mol. Biol.* **2007**, *373*, 153.
(8) Sulkowska, J. I.; Sulkowski, P.; Onuchic, J. *Proc. Natl. Acad. Sci. U.S.A.* **2009**, *106*, 3119.
(9) Bolinger, D.; Sulkowska, J. I.; Hsu, H. P.; Mirny, L. A.; Kardar, M.; Onuchic, J. N.; Virnau, P. *PLoA Comput. Biol.* **2010**, *6*, No. e1000731.
(10) Kolesov, G.; Virnau, P.; Kardar, M.; Mirny, L. A. C. P. *Nucleic Acids Res.* **2007**, *35*, W425.
(11) Lai, Y.-L.; Yen, S.-C.; Yu, S.-H.; Hwang, J.-K. *Nucleic Acids Res.* **2007**, *35*, W420.

(12) Lai, Y. L.; Chen, C. C.; Hwang, J. K. *Nucleic Acids Res.* **2012**, *40*, W228.
(13) Lua, R. C.; Grosberg, A. Y. *PLoS Comput. Biol.* **2006**, *2*, e45.
(14) Virnau, P.; Mirny, L. A.; Kardar, M. C. P. *PLoS Comput. Biol.* **2006**, *2*, e122.
(15) Mallam, A. L.; Jackson, S. E. *Structure (London, U.K.)* **2007**, *15*, 111.
(16) Noel, J. K.; Sulkowska, J. I.; Onuchic, J. N. *Proc. Natl. Acad. Sci. U.S.A.* **2010**, *107*, 15403.
(17) Alam, M. T.; Yamada, T.; Carlsson, U.; Ikai, A. C. P. s. *FEBS Lett.* **2002**, *519*, 35.
(18) Sulkowska, J. I.; Sulkowski, P.; Szymczak, P.; Cieplak, M. *Proc. Natl. Acad. Sci. U.S.A.* **2008**, *105*, 19714.
(19) Sulkowska, J. I.; Rawdon, E. J.; Millett, K. C.; Onuchic, J. N.; Stasiak, A. *Proc. Natl. Acad. Sci. U.S.A.* **2012**, *109*, E1715.
(20) Sulkowska, J. I.; Noel, J. K.; Onuchic, J. N. *Proc. Natl. Acad. Sci. U.S.A.* **2012**, *109*, 17783.
(21) Mallam, A. L.; Jackson, S. E. *J. Mol. Biol.* **2005**, *346*, 1409.
(22) Mallam, A. L.; Jackson, S. E. *J. Mol. Biol.* **2007**, *366*, 650.
(23) Yeates, T.; Norcross, T. S.; King, N. P. *Curr. Opinion Chem. Biol.* **2007**, *11*, 595.
(24) Mallam, A. L.; Morris, E. R.; Jackson, S. E. *Proc. Natl. Acad. Sci. U.S.A.* **2008**, *105*, 18740.
(25) Mallam, A. L.; Onuoha, S. C.; Grossmann, J. G. n.; Jackson, S. E. *Mol. cell* **2008**, *30*, 642.
(26) Faisca, P. F. N.; Travasso, R. D. M.; Charters, T.; Nunes, A.; Cieplak, M. *Phys. Biol.* **2010**, *7*, No. 16009.
(27) Li, W. F.; Terakawa, T.; Wang, W.; Takada, S. *Proc. Natl. Acad. Sci. U.S.A.* **2012**, *109*, 18625.
(28) Mallam, A. L.; Jackson, S. E. *Nat. Chem. Biol.* **2012**, *8*, 147.
(29) Beccara, S. A.; Skrbic, T.; Covino, R.; Micheletti, C.; Faccioli, P. *PLoS Comput. Biol.* **2013**, *9*, No. e1003002.
(30) Soler, M. A.; Faisca, P. F. N. *PLoS One* **2013**, *8*, No. e74755.
(31) Sulkowska, J. I.; Sulkowski, P.; Szymczak, P.; Cieplak, M. *J. Am. Chem. Soc.* **2010**, *132*, 13954.
(32) Keller, J.; Leulliot, N.; Cambillau, C.; Campanacci, V.; Porciero, S.; Prangishvili, D.; Forterre, P.; Cortez, D.; Quevillon-Cheruel, S.; Tilbeurgh, H. *Virol. J.* **2007**, *4*, 10.
(33) He, C. Z.; Genchev, G. Z.; Lu, H.; Li, H. B. *J. Am. Chem. Soc.* **2012**, *134*, 10428.
(34) Cao, Y.; Lam, C.; Wang, M. J.; Li, H. B. *Angew. Chem., Int. Ed.* **2006**, *45*, 642.
(35) Cao, Y.; Li, H. B. *Nat. Mater.* **2007**, *6*, 109.
(36) Marko, J. F.; Siggia, E. D. *Macromolecules* **1995**, *28*, 8759.
(37) Bell, G. I. *Science* **1978**, *200*, 618.
(38) Evans, E.; Ritchie, K. C. P. *Biophys. J.* **1997**, *72*, 1541.
(39) Carrion-Vazquez, M.; Oberhauser, A. F.; Fowler, S. B.; Marszalek, P. E.; Broedel, S. E.; Clarke, J.; Fernandez, J. M. *Proc. Natl. Acad. Sci. U.S.A.* **1999**, *96*, 3694.
(40) Rief, M.; Fernandez, J. M.; Gaub, H. E. *Phys. Rev. Lett.* **1998**, *81*, 4764.
(41) Phillips, J. C.; Braun, R.; Wang, W.; Gumbart, J.; Tajkhorshid, E.; Villa, E.; Chipot, C.; Skeel, R. D.; Kale, L.; Schulten, K. *J. Comput. Chem.* **2005**, *26*, 1781.
(42) MacKerell, A. D.; Bashford, D.; Bellott, M.; Dunbrack, R. L.; Evanseck, J. D.; Field, M. J.; Fischer, S.; Gao, J.; Guo, H.; Ha, S.; Joseph-McCarthy, D.; Kuchnir, L.; Kuczera, K.; Lau, F. T. K.; Mattos, C.; Michnick, S.; Ngo, T.; Nguyen, D. T.; Prodhom, B.; Reiher, W. E.; Roux, B.; Schlenkrich, M.; Smith, J. C.; Stote, R.; Straub, J.; Watanabe, M.; Wiorkiewicz-Kuczera, J.; Yin, D.; Karplus, M. *J. Phys. Chem. B* **1998**, *102*, 3586.
(43) Mackerell, A. D., Jr.; Feig, M.; Brooks, C. L., III *J. Comput. Chem.* **2004**, *25*, 1400.
(44) Humphrey, W.; Dalke, A.; Schulten, K. *J. Mol. Graphics Modell.* **1996**, *14*, 33.
(45) Paci, E.; Karplus, M. *Proc. Natl. Acad. Sci. U.S.A.* **2000**, *97*, 6521.
(46) Haberthur, U.; Caflisch, A. *J. Comput. Chem.* **2008**, *29*, 701.
(47) Peng, Q.; Li, H. B. *Proc. Natl. Acad. Sci. U.S.A.* **2008**, *105*, 1885.
(48) Guo, Z. Y.; Thirumalai, D. *Biopolymers* **1995**, *36*, 83.
(49) Hagen, S. J.; Hofrichter, J.; Szabo, A.; Eaton, W. A. *Proc. Natl. Acad. Sci. U.S.A.* **1996**, *93*, 11615.
(50) Lu, H.; Isralewitz, B.; Krammer, A.; Vogel, V.; Schulten, K. *Biophys. J.* **1998**, *75*, 662.
(51) Lu, H.; Schulten, K. *Proteins: Struct., Funct., Genet.* **1999**, *35*, 453.
(52) Carrion-Vazquez, M.; Marszalek, P. E.; Oberhauser, A. F.; Fernandez, J. M. *Proc. Natl. Acad. Sci. U.S.A.* **1999**, *96*, 11288.
(53) Rico, F.; Gonzalez, L.; Casuso, I.; Puig-Vidal, M.; Scheuring, S. *Science* **2013**, *342*, 741.
(54) Wang, T.; Ikai, A. *Jpn. J. Appl. Phys., Part 1* **1999**, *38*, 3912.
(55) Bornschlogl, T.; Anstrom, D. M.; Mey, E.; Dzubiella, J.; Rief, M.; Forest, K. T. *Biophys. J.* **2009**, *96*, 1508.
(56) Dzubiella, J. *J. Phys. Chem. Lett.* **2013**, *4*, 1829.
(57) Sulkowska, J. I.; Sulkowski, P.; Szymczak, P.; Cieplak, M. C. *Phy. Rev. Lett.* **2008**, *100*, No. 058106.